12-11-2013

Feed Rate Effects In Freeform Filament Extrusion

Omkar Rishi

ROCHESTER INSTITUTE OF TECHNOLOGY

Feed Rate Effects In Freeform Filament Extrusion

OMKAR RISHI

12/11/2013

Thesis submitted to the Faculty of the

Rochester Institute of Technology

In partial fulfillment of the requirements for the degree of

Master of Science in Industrial Engineering

Department of Industrial and Systems Engineering

Thesis Committee

Dr. Denis Cormier

Dr. Marcos Esterman

Department of Industrial and Systems Engineering

Kate Gleason College of Engineering

Rochester Institute of Technology

CERTIFICATE OF APPROVAL

Dec , 2013

M.S. DEGREE THESIS

The M.S. Degree Thesis of Omkar Rishi

has been examined and approved by the

thesis committee as satisfactory for the

thesis requirement for the

Master of Science degree

Approved by:

Dr. Denis Cormier, Thesis Advisor

Dr. Marcos Esterman, Committee Member

Abstract

3D printing technologies have evolved drastically in the last decade. Professional grade 3D printers produce very high quality parts largely because they have been optimized for use with just a few different materials and do not allow the user to change process parameters. Conversely, Freeform Filament Extrusion (FFE) is a technology that has emerged as a favorite of hobbyists due to widespread availability of low cost open architecture machines that permit extensive experimentation with any number of materials. The FFE 3D printing process operates by feeding thermoplastic filament through a heated nozzle while the nozzle "draws" the desired pattern one layer upon the next. The output from these hobby style FFE 3D printers is often less than ideal in large part because users lack an understanding of how critical process parameters affect the speed and diameter of polymer filament as it exits the nozzle.

This research focuses on the issue of unwanted deformation of the extruded polymer during 3D printing. As a first step, the feeding mechanism of an FFE 3D printer was studied in order to find the slippage (loss) between the feeding mechanism and the filament. The relationship between feed screw rotational speed and and volumetric flow rate through the nozzle tip was then established. With known volumetric flow rates, the cross sectional profiles of printed lines were measured using a laser profilometer. This information provides an indication of suitable nozzle head translation speeds for each feed screw rotational speed. Lastly, this study considers the effect of die swell in the extrusion process and concludes that the stand-off distance should be varied to avoid unwanted deformation of the extruded filament.

Acknowledgements

I would sincerely like to express my gratitude to all who supported and helped me to complete my thesis.

First and foremost, I would like to thank my parents Snehal and Mohan Rishi and my brother Aniket for their unconditional love and perpetual support. Without their unwavering faith, graduation would never have been possible.

I would like to thank my primary advisor Dr. Denis Cormier for his constant guidance and encouragement. Without his inputs this thesis would not have been possible. I would also like to thank Dr. Marcos Esterman for his patience and invaluable guidance throughout my thesis. I am grateful to have had an opportunity to learn from both.

I would like to thank my friend and lab mate Chaitanya who has proactively offered assistance throughout my academic and personal life. I would like to extend my gratitude to my friends Anirudha, Atul, Amey, Anshul, Nisharth and Mugdha for making my stay at Rochester enjoyable and memorable. I also owe my friends Priyanka and Mufaddal for their constant encouragement. Lastly, I am profoundly thankful to God for everything he has blessed me with.

Table of Contents

List of Figures

List of Tables

1. Introduction

1.1 Rapid Prototyping

Rapid prototyping is a process that creates physical 3D solid models by adding material layer by layer. Rapid prototyping machine can manufacture components within a few hours without any need to produce molds or dies. This reduces overall product development time and increases manufacturing flexibility.

There are a number of steps involved in order to print a part on a rapid prototyping machine. Initially, a part is modeled using three-dimensional computer aided design (CAD) software such as Solidworks. Three-dimensional models are saved in the STL file format which is commonly used by all rapid prototyping machines. Each machine comes with model slicing software which determines a variety of process parameter values. The STL file is first imported into the machine's slicing software. The STL file is then positioned and oriented, and the part size is adjusted as needed. The STL file is then sliced into a number of layers. Each sliced layer has a cross sectional area of finite thickness. During the slicing process, process parameters such as part material, material fill density, and number of contours are adjusted as needed. Finally the build file is generated and transferred to the rapid prototyping machine. The machine reads this build file and automatically constructs the part under minimal supervision. The part is built layer by layer, where each layer is a cross sectional slice of desired thickness. Once a given layer is printed, the build platform lowers by the distance equal to the slice layer thickness. With the lowered build platform, the next layer is built on top of the previous layer. This process continues until the build is complete.

Figure 1 illustrates printed layers in a sequential part printing process. Once the part is built, it should be removed carefully from the machine. The removed part often needs post processing such as support material removal, surface finishing or part coloring depending on the machine that was used for printing. With careful post processing, the part is finally ready for its intended

application. The quality of a printed part depends on process settings involving slicing technique, layer thickness, etc.

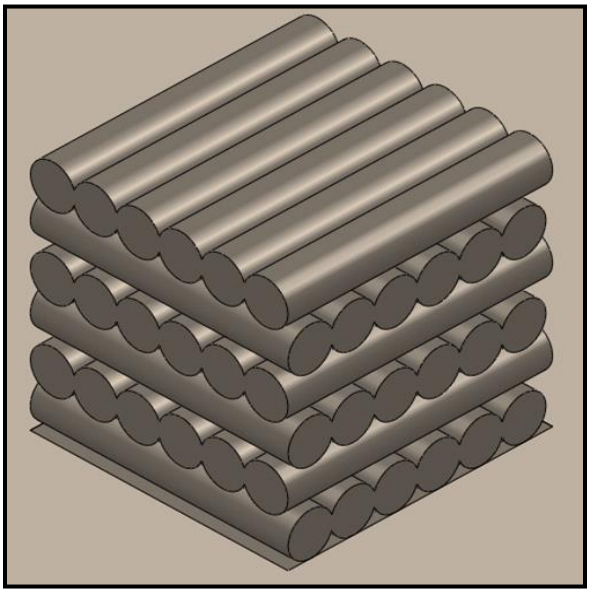

Figure 1: Layers being added up in part printing process

Rapid prototyping processes are able to process a variety of materials including metals, polymers, and ceramics. These materials can come in various forms such as solid sheets, thermoplastic filaments, powder, or photopolymer resin. The major rapid prototyping technologies include Stereolithography (STL), Selective Laser Sintering (SLS), and Fused Deposition Modeling (FFE) (Yan & Gu, 1996).

Rapid Prototyping is widely used in the product development process. Rapid prototyping does not need special tooling or dies to manufacture parts. Consequently, creating a prototype is much easier, cheaper and faster compared with conventional production methods. Rapid prototyping also improves product flexibility and hence can satisfy individual customer demands. The ability to manufacture functional parts is also useful in carrying out testing to a certain extent (Chua, Leong, & Lim, 2010).

1.2 Freeform Filament Extrusion

Freeform Filament Extrusion (FFE) is the generic name for Stratasys' original Fused Deposition Modeling (FFE) process. FFE is one of the most widely used and commercially available rapid prototyping technologies in existence. In the FFE process, thermoplastic filament is fed into a heated nozzle whose temperature exceeds the glass transition temperature of the feedstock. The resulting soft polymer is extruded through the nozzle. An XY gantry moves the nozzle over the prescribed toolpath as material is extruded, thus "printing" one layer of material. The process is repeated one layer on top of another to manufacture 3D solid model. The thickness of each sliced cross section identifies the number of layers in a 3D model. With a known number of layers and part build orientation, the total part building time is computed. In FFE, a variety of materials can be used such as investment casting wax, acrylonitrile butadiene styrene (ABS), and nylon to build a part. Support material may also be printed beneath downward-facing surfaces. Polylactic acid (PLA) is often used as a support material. Most commonly, ABS is used to build a part whereas PLA is used as a support material. As PLA is a water soluble polymer, it can be easily removed in warm water with a mild detergent.

In the FFE process, softened polymer flows through a nozzle that is translated along a prescribed path over a build platform. The deposited material solidifies very quickly. Once the layer is formed, the build platform lowers by an amount equal to the layer thickness so that the next layer can be printed. With the help of numerically controlled stages, the movement of the nozzle (deposition head) and the building platform is controlled in the horizontal and vertical directions respectively. Most FFE systems have two extrusion nozzles – one for the structural build material and one for the removable support material. Once the part is completed, it is carefully removed from the build plate.

Extrudable thermoplastics are available in a variety of colors. Additionally, thermoplastics are cheap and safe to use. The build volume of most FFE machines is relatively small, hence they are most commonly used as desktop prototyping machines (Masood, 1996), (Pham & Gault, 1998), (Yan & Gu, 1996).

Figure 2 shows the overall FFE process. As explained in the previous paragraph, thermoplastic filament is passed through the heated barrel to melt the material. This molten material passes through the nozzle onto the build platform. The print head moves in the X-Y plane whereas build platform moves in the Z direction.

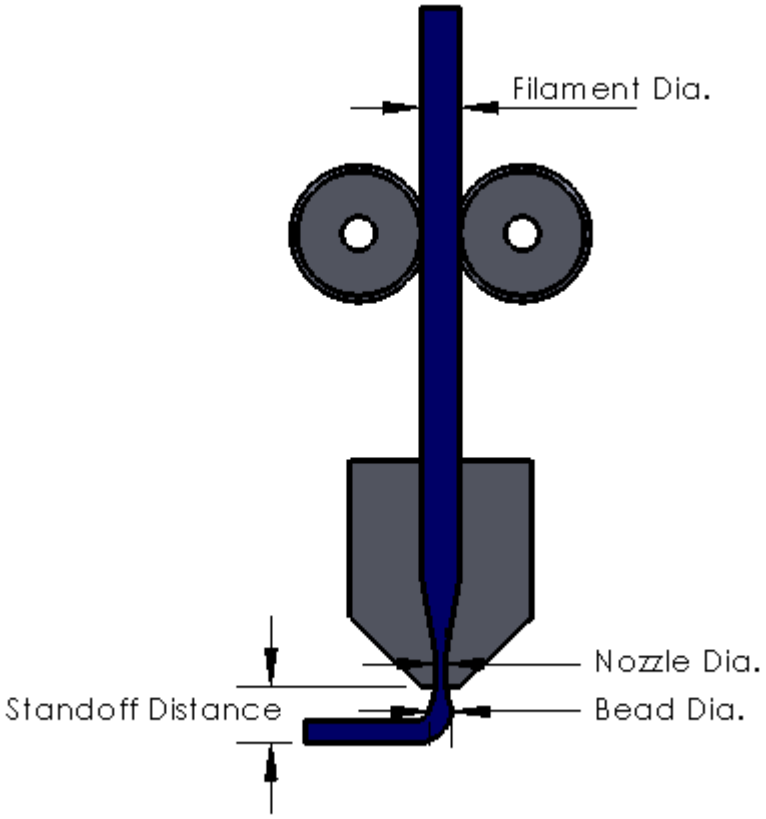

Figure 2: Schematic of FFE

Stratasys Inc. is the chief manufacturer of commercially available high end FFE machines. Following the expiration of Stratasys' original FFE patent, a range of low cost FFE machines were introduced. These include the Dimension U-Print, Makerbot, RepMan 3.1, BFB 3000, and so on.

One of the biggest advantages of using FFE is that one can print durable parts with a variety of materials. Furthermore, the small size allows these systems to be used in office environments. However, there are a number of challenges associated with FFE. As this technique prints one

layer on top of another, seam lines are observed between two layers of printed material. Figure 3 shows a micrograph of printed layers in which gaps between layers are clearly visible in some areas. These voids can reduce density and strength of the parts. For overhanging geometries, the printing of supports leads to additional build time and material wastage. Build time can be reduced through the use of thicker layers, however, surface quality deteriorates as layer thickness increases.

In summary, the FFE process has been widely credited as the driving force behind the huge surge of interest in 3D printing and additive manufacturing in recent years. Earlier commercial systems had closed architectures with a very small number of materials. These systems were specifically geared towards commercial users, and the closed nature of these systems greatly facilitated the task of building quality parts. The recent proliferation of low cost open architecture 3D printers has opened the doors to hosts of hobbyists and inventors who are more interested in experimenting with the process than they are in building production parts. There is therefore a need to better understand the relationships between process parameter values and the resulting print output. The remainder of this document focusses on a study of the FFE process and possible techniques to improve the quality of parts produced in low cost hobby style FFE machines that have started to proliferate.

Figure 3: The micrograph showing the gap between printed layers

2 Literature Review

The principle of FFE is relatively simple on the surface of things. Heated plastic is extruded through a nozzle as the nozzle moves over a platform. Even if the process appears to be simple, there are a number of subtle issues that can significantly affect print quality. There has been extensive research work on improving FFE process. Most of the research focuses has been on new material development for FFE. There has also been significant research dedicated to improving part accuracy and surface quality.

2.1 Part Dimensional Accuracy

One of the important aspects of a part is its dimensional accuracy. Hoekstra *et al.* (2005) studied the dimensional accuracy of ABS parts produced via the FDM process. Dimensions were measured with a coordinate measuring machine and digital micrometer. This experiment led to the conclusion that part size, location of the part in work envelope, and envelop temperature each had a significant effect on the dimensional accuracy printed parts (Hoekstra, Pennington, & Newcomer, 2005).

Saquib *et al.* (2012) printed thick and thin wall cylinders to study the effect of part position on the build platform, layer thickness and part orientation. They measured cylindricity, perpendicularity, and flatness with the help of a coordinate measuring machine (CMM). They came to the conclusion that form and feature interfaces affect the part accuracy more than the process parameter settings (Saqib & Urbanic, 2012).

The shrinkage of FDM materials can also have a significant effect on part dimensional accuracy. In order to quantify the effect of shrinkage on a part's dimensional accuracy, it is necessary to know the shrinkage in all dimensional axes. Research on the dimensional accuracy of parts conducted by Sood *et al.* (2009) addresses this issue using the Grey Taguchi Method. They printed rectangular blocks to study the influence of layer thickness, part orientation, raster angle, road width and air gap. They suggested optimum values for these factors to improve overall dimensional accuracy of printed parts (Sood, Ohdar, & Mahapatra, 2009).

2.2 Part Surface Finish

A high quality surface finish improves both the aesthetics and material properties of a 3D printed component. Various methods have been suggested over the years to improve the surface quality of parts fabricated by FFE. Vasudevarao *et al.* (2000) studied the effect of FFE process parameters on the printed part's surface finish. Parts were printed with up facing angles, and process parameters including build orientation, layer thickness, road width, air gap and temperature were studied. They came to the conclusion that printed layer thickness and part orientation affect the surface finish the most (Vasudevarao, Natarajan, Henderson, & Razdan, 2000).

In order to improve the surface finish, a variety of post processing techniques have been proposed. Galantucci *et al.* (2009) suggested that CAD model slicing height and raster width are the main factors that affect the quality of surface finish. Additionally, the authors suggested that chemical post processing improved surface finish at the small expense of part size (Galantucci, Lavecchia, & Percoco, 2009).

Another study carried out by Pandey *et al.* (2003) suggested that in order to improve the surface finish, it is necessary to reduce the stair stepping effect. The authors proposed a material removal technique involving hot cutter machining (HCM) and demonstrated that functional parts with improved surface finish could be fabricated (Pandey, Venkata Reddy, & Dhande, 2003).

2.3 Process Optimization

It is a well-known fact that Rapid Prototyping processes can drastically reduce the lead time of a new product launch. Furthermore, these processes can significantly reduce the cost of designing and manufacturing complex parts. However, fabricating dimensionally accurate, large complex parts with a smallest possible layer thickness can hours or sometimes even days. So optimizing the FFE process is an absolute necessity (Han, Jafari, & Seyed, 2003). There have

been a number of process optimization efforts aimed at reducing part building time, minimizing support material, improving the CAD model slicing process, etc.

For reducing part build time, Han *et al.* (2003) proposed a concept of printing a part with multiple layer thicknesses. Additionally they proposed an increase in the printing head speed and road width. While studying these parameters they concentrated on maintaining surface finish quality (Han et al., 2003).

Another approach to reduce part build time is to eliminate or minimize support structure. Building an overhanging structure below which support structure must be printed is a time consuming process. So eliminating or reducing support structure where possible is recommended. In order to address this issue, Yang *et al.* (2003) proposed a multi-orientational deposition method (MOD). MOD incorporates an additional degree of freedom in the build platform so that it can rotate on the Z-axis along with the laterally oriented deposition head. This new method resulted in reduced build time and improved material utilization (Yang, Fuh, Loh, & Wong, 2003).

2.4 Part Strength

Building parts with acceptable compressive and tensile strength is one of the necessities for any process. There have been a number of efforts to improve the part strength of FFE parts. One such effort was undertaken by Ahn *et al.* (2002). They used ABS to fabricate parts on a Stratasys FDM 1650 machine. Raster orientation, air gap, bead width, color and model temperature were studied. Printed parts were tested for tensile and compressive strength, and the results were compared with injection molded parts. From the experimental results, the authors formulated the set of guidelines to improve the part strength and part accuracy (S. H. Ahn, Montero, Odell, Roundy, & Wright, 2002).

Bellini *et al.* (2003) demonstrated that part orientation and print direction were the most dominant factors in improving part strength (Bellini & Güçeri, 2003). Lee *et al.* (2007) conducted research on compressive strength of three rapid prototyping processes. They carried

out tests on parts fabricated using ABS in different nozzle scan directions viz. axial, transverse and diagonal. They came to the conclusion that FFE parts fabricated with an axial build direction has the highest compressive strength (Lee, Kim, Kim, & Ahn, 2007). Research conducted by Sood *et al.* (2012) showed that along with part orientation (build direction), the layer thickness, raster angle, raster width and air gap also affect the compressive strength of the part (Sood, Ohdar, & Mahapatra, 2012).

2.5 Research Objectives

In the past, many researchers have worked on improving the properties of printed parts such as surface finish, dimensional accuracy, tensile strength, etc. These researchers have primarily focused on finding the best process parameters for the final product using closed architecture systems in which the user had relatively little control over the process parameter values. Relatively few researchers have worked on modeling the fundamentals of the printing process. Hence there exists a need to study the printing process where extruded filament fails to meet expected results. This research focuses on some of these issues and aims to establish a process to be followed in order to predict the output of an FFE extrusion head. The research focuses on modeling the relationship between filament feed rate and the recommended suitable range of nozzle head translation speed and stand-off distance that will produce a desirable printed bead. Further this research also models the die swell phenomena that takes place in the FFE extrusion process.

3 Research Methodology

3.1 Methodology

In studying prior research on the FFE process, it has been found that most of the experiments were conducted on commercially available FFE machines. There has been very little research on recently introduced open-architecture FFE machines. The open nature of these machines gives experimenters access to the full range of process parameters such as extruder temperature, filament feed rate, nozzle translation speed, and stand-off distance while working with new materials not previously available. The BfB 3000 FFE machine was chosen as the test platform for this research. This machine provides users with full access to the aforementioned process parameters, hence enabling a very comprehensive experiments to be performed (Helmer & Mobbs, 2011).

ABS plastic is very well known for its compatibility with the FFE process. The BfB 3000 machine uses 3 mm diameter filament feedstock materials that are available in a wide variety of colors. In order to eliminate color as a potential source of process variability, blue ABS filament was arbitrarily chosen as the feedstock material for all experiments. As a first step, it was necessary to verify the density of ABS blue filament chosen for this work. The density of ABS blue was verified with the help of Archimedes principle and other mathematical calculations.

Screening experiments were also performed in order to determine upper and lower parameter value ranges for subsequent experiments. In screening experiments, straight 100 mm long lines were printed by varying the basic process parameters of speed multiplier, flow rate, extruder head temperature, and stand-off distance. In some of the printed lines, conditions leading to either insufficient or excessive extrudate velocity relative to the nozzle scanning velocity were observed. These two conditions manifest themselves as either broken printed lines (i.e. gaps) or printed lines in which so much material comes out that it is smeared by the print nozzle.

In order to address these issues, the filament feeding mechanism of the BfB-3000 extrusion head was analyzed. The blue ABS filament was extruded for 100 seconds by varying the

filament feed screw rotational speed and extrusion nozzle temperature. For each experimental condition, extruded filaments were collected in aluminum weigh cups in order to determine the mass of material extruded during the 100 second time period. With known mass and density, the volumetric flow rate of extruded filament in mm^3/min was calculated and compared with the expected flow rate to determine whether or not slippage was occurring in the filament feeding mechanism.

As a next step, the flow rate at the extruder tip was correlated with the nozzle head translation speed. Straight 100 mm long lines were printed at specific nozzle head translation speeds while keeping the filament feed screw rotational speed constant. The extrusion nozzle temperature was kept at 260^oC. Using a Keyence IL-030 laser profilometer, the width and height of each printed line was measured at three locations. The profilometer measurements were logged into an Excel spreadsheet to allow the cross sectional area of each line scan to be calculated. The cross sectional area (mm^2) was multiplied by nozzle head translation speed (mm/min) to calculate the estimated volumetric flow rate (mm^3/min) of material coming out of the nozzle tip. A comparison of calculated flow rates with actual flow rates identifies the processing conditions where the filament feed-in mechanism begins to slip. Likewise, mathematical models and experimental results are used to identify the suitable range of nozzle head translation speeds for each feed screw rotational speed.

Die swell is a phenomenon where viscoelastic material exiting a die opening will swell to some diameter that is larger than the die opening due to recoverable strain in the material. In order to quantify the die swell effect in the FFE process, the previously extruded samples were used. The diameter of extruded filament was measured with the help of a digital caliper. The diameter of filament exiting the nozzle should logically affect the recommended gap between the nozzle and the print substrate. As the diameter increases, the gap should likewise increase. Failing to adjust the gap size can lead to smearing of the printed bead if the gap is smaller than the extrudate diameter.

3.2 The BfB 3000 Machine

Figure 4 shows the main parts of the BfB 3000 printer. As shown in the figure, the BfB 3000 has a simple structure and fits on a desktop. The model used in these experiments has three extruders and hence can print up to three different materials in a single layer. Generally, one of the extruders is used to extrude the support material. The overall dimensions of this printer are 515 x 515 x 598 mm, and the overall weight is around 38 kg. The maximum size of the parts that can be built in this triple head printer is 185 x 275 x 201 mm. The maximum temperature that the printing head (nozzle) can achieve is 270^{o}C. Thermoplastics that can be printed using BfB 3000 include ABS, PLA or soluble clear translucent PLA.

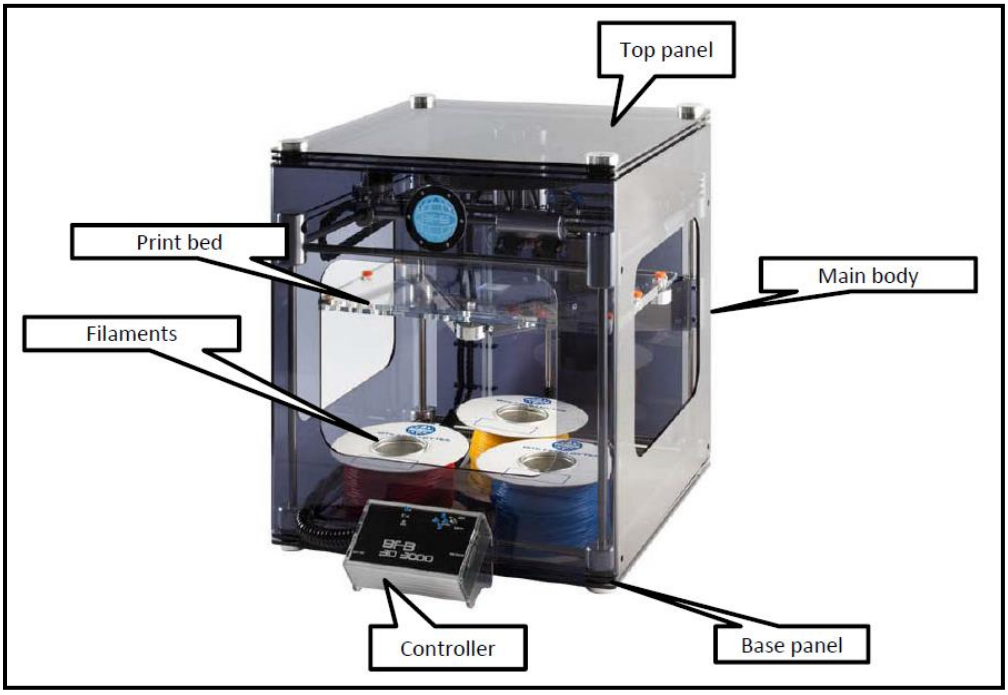

Figure 4: Nomenclature of BFB 3000

The BfB 3000 prints 3D models by depositing one layer on the top of the other layer. In order to start printing, it is necessary to carry out few preprinting procedures. As a first step, it is necessary to level the build platform within 0.1 mm accuracy. Following platform leveling, all three print heads are adjusted to make sure that they are at the same height with respect to machine build platform. Once these adjustments are done, the machine is ready to print.

During preprocessing, it is necessary to create a three dimensional solid model and save it in the STL file format. Using the Axon slicing software provided with the machine, the STL file is sliced using the specified layer thickness and filling pattern. This sliced file is then saved in the BfB file format which contains machine readable G codes. This G code file is then transferred to an SD memory card which is inserted in the controller of the BfB 3000. The machine reads the file and executes printing instructions from it. The machine first goes to its home position and starts to heat up the extruders. Once the set point temperature is achieved, the printing commences. The BfB 3000 first prints the contour of that layer's geometry and then fills in the contour as per the selected filling pattern. After completion of the first layer, the build platform is lowered by an amount equal to the slice layer thickness in order to print a second layer on top of the first layer. This process continues until the last layer is printed.

3.3 Process Parameters in the BfB 3000

Every process is affected by controllable and non-controllable parameters. So to list down these parameters is the first step in any experiment. The following factors can be controlled while using the BfB 3000 machine.

Speed Multiplier: This is a factor that increases or decreases the nominal nozzle scan speed in the XY plane. With a higher speed multiplier, the print head moves at a faster speed and hence lowers the part building time. Speed multiplier is a continuous variable that can be varied the Axon software interface from 0.5X to 3.0X in increments of 0.1. It is also possible to map the Speed Multiplier value to a nozzle head translation speed in the Axon software generated BfB code file. The BfB code file contains G-code and M-code instructions for the tool head. A speed multiplier of 0.5X corresponds to a nozzle head translation speed of 480 mm/min, while a speed multiplier value of 3.0X corresponds to 2880 mm/min. Lastly, it is possible to directly edit the nozzle head translation speed in the G-code file to values between 100 mm/min and 2880 mm/min. For screening experiments, the speed multiplier was varied between 0.5X (480 mm/min) and 1.5X (1440 mm/min).

Feed Screw Speed: Feed screw speed controls the rate at which the liquefied thermoplastic flows through the nozzle tip. Within the BfB's extrusion head, the filament is pushed up against a rotating screw using spring loaded thrust bearings. The rotating screw threads exert a downward force that pushes the thermoplastic filament into the heater barrel. The filament feed rate is therefore a function of drive screw rotational rate (rev/min). The higher the screw speed, the higher the filament feed rate. As filament feed rate increases, the volumetric flow rate of plastic extruded from the nozzle increases as well. In the BfB 3000, the drive screw speed can be varied from 0 to 230 rev/min (revolutions per minute). 0 rev/min indicates no material is fed-in whereas 230 rev/min indicates the maximum material flow rate.

Nozzle Temperature: This is desired processing temperature for the thermoplastic filament prior to extrusion. In the BfB 3000, the maximum allowable nozzle temperature is 270^{o}C. Above 270^{o}C, it can potentially damage the apparatus.

Stand-off Distance: This is the distance between the extruder tip and the building platform. If the stand-off distance is too large, then the material flowing out of the extruder tip starts to curl before making contact with and adhering to the substrate. Excessive stand-off distance also causes poor adhesion of the part with the base plate. On the other hand, very small stand-off distances can result in smearing of the extruded material by the extruder tip. This also generates a great deal of back-pressure that lowers the volumetric flow rate. So for reliable and good quality printing, the stand-off distance must be adjusted and maintained throughout the printing process.

The nozzle head translation speed, feed screw speed, nozzle temperature and stand-off distance are the primary non-geometric process parameters that can be varied while printing. Other than these four factors, there are several other print geometry factors such as part fill density, part fill pattern, and part slicing layer thickness that can be controlled during printing. Along with these controllable factors, there are other factors that are more difficult to control with the BfB 3000. One of these factors is part surrounding temperature or envelop temperature. The BfB 3000 does not use an enclosed build chamber. Consequently, the temperature in the build chamber is largely determined by the room temperature. Another

factor is nozzle diameter. The BfB 3000 nozzle (and hence nozzle diameter) is fixed and cannot be swapped. In order to change the nozzle diameter, the entire nozzle head assembly would need to be replaced. The standard nozzle diameter for the BfB 3000 is 0.5 mm. Lastly, the part printing location on the build platform was kept constant throughout experimentation. Samples were printed at the center of the build platform.

3.4 Measurement

For measurement purposes, two different measuring instruments were used.

1. A&D HR-60 analytical balance

   The HR-60 analytical balance was used for measuring the mass of extruded filaments. The HR-60 analytical balance has a weighing capacity of 60 grams with a resolution of 0.0001 gram.

2. Keyence IL-030 laser profilometer

   The IL-030 laser profilometer was used to measure the cross sectional profile of printed beads. With the help of an amplifier unit, the IL-1000, and a serial communication unit, a DL-RS1A laser unit was set up. The substrate was linearly translated at constant velocity beneath the laser such that the laser scan direction was perpendicular to the printed line orientation. The output from the system was logged into an MS Excel spreadsheet. This was used to calculate the height and width of the printed beads as well as the cross sectional area. This laser profilometer has the measurement range of between 20 to 45 mm between the measurement head and the sample being scanned. The stated repeatability is 1 µm. The spot diameter of the IL-030 at the standard distance is approximately 200 × 750 µm.

4 Experimental Results and Analysis

4.1 Verification of the density of blue ABS

Before proceeding with experimentation, it was necessary to measure the density of the ABS blue filament used for experimentation. The nominal density of ABS (D_{ABS}) is given as:

D_{ABS} = 1.04 gm per cubic cm (At 70 ^{O}F)

Experiments were conducted to determine whether the ABS blue filament has a comparable density. In the first experiment, the density of ABS blue was calculated using Archimedes principle. In order to perform this experiment, the ABS blue filament of length equal to 900 mm was cut from the bundle. This filament was then cut into small pieces and weighed on the HR-60 analytical balance (m_{ABSC}). Then a graduated cylinder was filled with water, and the volume of filled water level was taken. The cut pieces of ABS blue filament were then submerged in the cylinder, and the new volume was observed. The difference between these two readings yields the volume of displaced water was calculated ($V_{displaced}$). With the help of Archimedes formula, the density of blue ABS (ρ_{ABSC1}) was calculated. Detailed results from the density experiments are as follows.

$$\rho_{ABSC1} = \frac{m_{ABSC}}{V_{Displaced}} \tag{4.1.1}$$

m_{ABSC} = 5.9007 gm

$V_{displaced}$ = 6 ml = 6 cm^3

$$\rho_{ABSC1} = \frac{5.9007\ gm}{6\ cm^3} = 0.98345\ {}^{gm}/_{cm^3}$$

In the second experiment, a mathematical approach was followed. As a first step, the blue ABS of known length (L_{ABS}) was cut from the bundle. Then the diameter of this wire formed ABS was measured at various locations and averaged (d_{ABS}) to ensure the uniform diameter of the ABS blue filament. With the known length and diameter of blue ABS, the volume of the ABS blue (V_{ABSV}) was calculated mathematically. Further this cut filament was weighed on the HR-60

analytical balance. With this known mass (M_{ABSV}) and volume, the density of the ABS blue (D_{ABSC2}) was calculated. Detailed calculations are as follows.

$$L_{ABS} = 762\ mm$$

$$d_{ABS} = 2.90\ mm$$

$$V_{ABSV} = \pi r_{ABS}{}^2 L_{ABS} \tag{4.1.2}$$

$$V_{ABSV} = \pi \left(\frac{2.90\ mm}{2}\right)^2 \times (762\ mm) = 5033.814\ mm^3 = 5.0338\ cm^3$$

$$M_{ABSV} = 5.2158\ gm$$

$$\rho_{ABSC2} = \frac{M_{ABSV}}{V_{ABSV}} \tag{4.1.3}$$

$$\rho_{ABSC2} = \frac{5.2158\ gm}{5.0338\ cm^3} = 1.036\ {}^{gm}/_{cm^3}$$

4.2 Screening experiments

Screening experiments were carried out in order to understand the effects of each process parameter on the overall part printing process. In the screening experiment, a single bead of blue ABS was printed on the build platform.

As discussed earlier, the screening experiments varied nozzle head translation speed, filament feed screw speed, nozzle temperature and stand-off distance. Each factor was varied between low and high values so that the interaction between two or more factors could be analyzed. Table 1 lists the process parameters and their respective lower and higher levels.

Table 1: Description of process parameter levels

Process Parameters	Lower Level	Higher Level
Speed Multiplier (X)	0.5	1.5
Flow rate (rev/min)	30	200
Nozzle Temperature (^{o}C)	250	270
Stand-off Distance (mm)	0.125	0.500

The main aim of the screening experiments was to find the factors which have the most pronounced effect on the profile of a printed layer. A full factorial experiment was conducted to find the effect of individual factors and interactions between them. The experiment consisted of 16 runs. Also these experiments were carried out in a randomized manner to minimize the effect of non-controllable factors. These single bead samples were printed on an unheated acrylic plate. To analyze the profile of the printed beads, the Keyence IL-030 laser profilometer setup was used. The output of the laser profilometer is recorded as a function of the distance of each point from the reference. These distance values are stored in the MS Excel spreadsheet. These values were plotted on in a graph in order to better visualize printed bead's measured cross section. These distance values are nothing but the height values of printed bead at a given X,Y location. The average of these height values was taken as a measure the bead height. The laser profilometer was scanned over each bead, and the height values were measured every 0.1 seconds. With known scanning speed (0.5082 mm/sec) and measurement frequency (1 measurement per every 0.1 sec), the distance between measurements is known to be 0.05082 mm. Since the reference height of the build plate is known, it is possible to identify the points where the laser first detects the printed line and then stops detecting the printed line. The distance between these two points yields the width of the bead. The details of this design of experiments and its results are tabulated in Table 2.

Table 2: Design of Experiments for Screening Experimentation

Std Order	Run Order	Speed Multiplier	Feed Screw Speed (rev/min)	Nozzle Temperature (°C)	Stand-off Distance (mm)	Average Height (mm)	Average Width (mm)
15	1	0.5X	200	270	0.500	0.828	3.147
2	2	1.5X	30	250	0.125	0.221	0.198
3	3	0.5X	200	250	0.125	0.809	3.167
8	4	1.5X	200	270	0.125	0.447	1.921
16	5	1.5X	200	270	0.500	0.449	1.913
12	6	1.5X	200	250	0.500	0.495	1.704
11	7	0.5X	200	250	0.500	0.831	3.254
5	8	0.5X	30	270	0.125	0.289	1.257
6	9	1.5X	30	270	0.125	0.176	0.716
10	10	1.5X	30	250	0.500	0.266	0.387
4	11	1.5X	200	250	0.125	0.466	1.759
14	12	1.5X	30	270	0.500	0.227	0.111
1	13	0.5X	30	250	0.125	0.331	1.166
7	14	0.5X	200	270	0.125	0.784	3.293
13	15	0.5X	30	270	0.500	0.087	0.988
9	16	0.5X	30	250	0.500	0.159	1.180

During these screening experiments, a number of important observations were made. In some cases, the head translation speed was too slow in relation to the rate at which material was extruded, resulting in excess material and smearing from the nozzle. In other cases, the head translation speed was too fast in relation to the rate at which material was extruded, resulting in stretching and breaking of the extruded bead. We can roughly associate these two conditions to the combination of factors used in screening experimentation. Typically, the stretching of an extruded bead can be observed in the cases of higher nozzle head translation speed (speed

multiplier), lower feed screw speed and higher stand-off distance. On the flip side, the smearing effect can be observed in cases where feed screw speed is higher and nozzle head translation speed (speed multiplier) is slower along with smaller stand-off distance. Furthermore, it was observed that at higher stand-off distance, the extruded bead was not able to stick to the build platform. Especially in case of higher translation speed, larger stand-off distance, lower temperature, and lower feed screw speed, the extruded bead did not stick properly to the build platform. In order to avoid these scenarios during printing, it is necessary to have the an appropriate balance between these process parameter values. In order to print the samples with precision and accuracy, it is necessary to understand and establish the relationships between between filament feed screw rotational speed and nozzle translation speed.

4.3 Filament feed rate versus extruder tip flow rate

Ideally, the extruder filament feed volumetric feed rate (cm^3/min) should be approximately equal to the volumetric flow rate of filament exiting the extruder tip (cm^3/min). In every mechanism, however, there are losses that will affect the actual flows. It is therefore necessary to assess the losses in any feeding mechanism.

This research focusses specifically on the BFB 3000, hence that feeding mechanism was studied. In the BFB 3000 machine, 3.0 mm (nominal) diameter ABS filament is fed into the heated extruder via a rotating feed-in screw. The rotational speed of this feed screw determine the feed screw rotational speed of the filament. The threads of the rotating screw are pressed against the plastic wire filament, thus exerting a downward force that pushes the filament into the heated nozzle. The rotational speed of the feed screw (rev/min) coupled with the pitch of the screw (mm/screw rotation) are converted into linear motion of filament (mm/min) which passes into the heated nozzle. The heated nozzle is set at a particular temperature that is appropriate for the thermoplastic material being printed. Due to the higher temperature in the barrel, the filament is heated above its glass transition temperature and softens. The soft polymer melt is subjected to force by solid plastic entering the heated barrel and thus is extruded through the extruder nozzle having a diameter of 0.5 mm. The rate at which material

exits the extruder tip is the printer's volumetric flow rate (cm^3/min). In order to establish a relationship between the filament feed screw rotational speed and the volumetric flow rate for the BfB 3000 extruder, the feed-in screw speed (rev/min) can be mathematically correlated to the linear speed of 3.0 mm diameter filament (mm/sec) going into the heated barrel. Using the filament's linear speed going in, one can establish a volumetric flow rate of plastic exiting the 0.5 mm diameter extruder tip using basic geometric calculations. Figure 5 shows the feeding mechanism of the BFB machine along with the terminology of each speed.

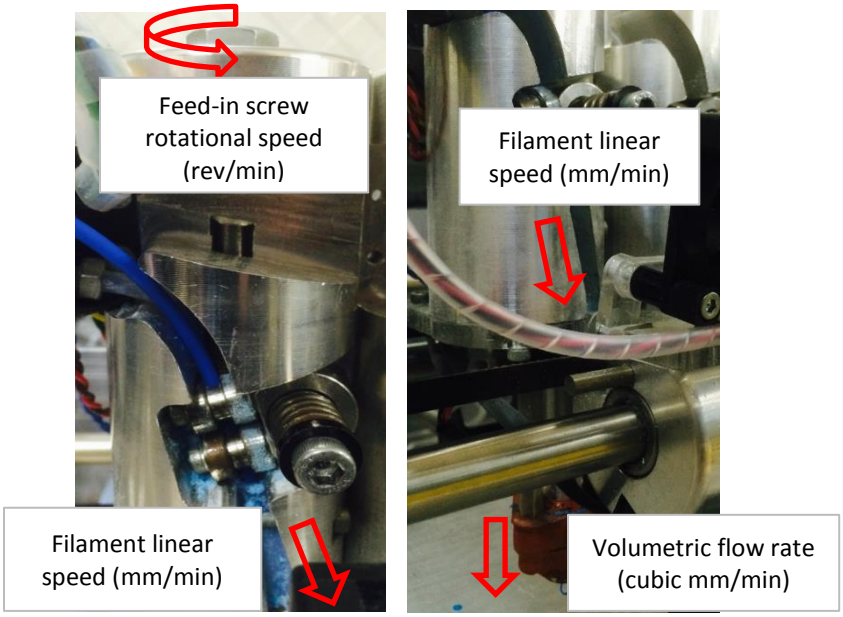

Figure 5: Feeding Mechanism of BFB-3000 and terminology used

In order to find the filament linear speed, simple geometrical calculations are performed. As shown in Figure 6, the angle between the feed-in screw's axis and the filament axis is denoted as ϑ. Further, the threads per millimeter of the feed screw is denoted as N_t. p denotes the vertical (Z-axis) pitch of the feed-in screw in mm/rev. With the simple right angle triangle geometry, the length of filament feed (L_f) in one revolution of feed-in screw can then be calculated.

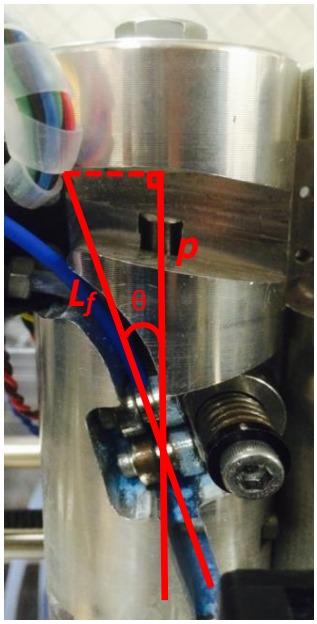

Figure 6: Right angle triangle geometry denoting the calculations of filament linear speed

The following calculations show the mathematical relationships as well as calculated filament linear speed ($L_{ABS\text{-}In\text{-}M}$) using measured values from the BfB 3000 system.

$\vartheta = 15^{o}$ (measured on BfB 3000 machine)

N_t = 1 thread/mm

$$p = \frac{1}{N_t} = 1\ {}^{mm}/_{rev}$$

For right angle triangle,

$$\cos\theta = \frac{p}{f_l} \tag{4.3.1}$$

$$L_f = \frac{p}{\cos\theta} = \frac{1}{\cos(15°)} = 1.0353\ {}^{mm}/_{rev}$$

To calculate the linear feed rate of filament (f_f), the feed screw revolution speed (N_f) should be multiplied by the length of passed over filament (L_f). Following sample calculations are for feed-in screw revolution speed of 15 rev/min.

$$f_f = N_f \times L_f \tag{4.3.2}$$

$$f_f = 15\ RPM \times 1.0353\ {}^{mm}/_{rev} = 15.5291\ {}^{mm}/_{min}$$

In order to test the validity of Eq. 3.6.2, a series of experiments were conducted. The extruder head of the BFB machine was raised well above the build platform, the filament was fed into the screw feed mechanism. The heated barrel was removed so that the only action of the head assembly was to feed filament without any back-pressure. This can be considered as a "no load" filament feed condition. With this modification, the screw feeder was rotated at different speeds, and filament was fed in for 60 seconds. After 60 seconds, the length of filament that had exited the nozzle assembly was measured. Diving this length by one minute gave the actual feed rate of filament (f_f) in mm/min. Table 3 shows the observed readings for each feed screw rotational speed in comparison with the mathematically predicted value.

Table 3: Feed screw speed versus calculated and actual filament feed rates

Feed Screw Rotational Speed (rev/min)	Calculated Filament Feed Rate (mm/min)	Actual Filament Feed Rate (mm/min)	Percent Difference (%)
15	15.5291	14.98	3.54
30	31.0583	30.01	3.38
60	62.1166	60.00	3.41
100	103.5276	100.04	3.37
150	155.2914	150.04	3.38
200	207.0552	200.06	3.38

As expected, the actual filament feed rate can be determined with reasonably good accuracy from the feed screw rotational speed. And hence from this step onwards, these values were used for further calculations.

In order to find the volumetric flow rate of plastic exiting the extruder tip, the next set of experiments was performed. Blue ABS filament was extruded through the nozzle for a time (t) of 100 seconds by varying the feed screw rotational speed (N_f) and the temperature of the nozzle (T_N). Table 4 shows the different feed screw rotational speeds and nozzle temperatures that were used for performing this set of experiment.

Table 4: Levels of feed screw rotational speed (rev/min) and Heating chamber temperature (^oC)

Feed-in screw revolution speed (rev/min)	Heating Chamber Temperature (^oC)
15	250
30	260
60	270
100	
150	
200	

For every possible combination of feed screw rotational speed (N_f) and nozzle temperature (T_N), 100 second's worth of extruded ABS filament was collected in aluminum foil cups so that the mass of extruded ABS (M_{ABS-E}) could be measured on a weigh scale. Sample mathematical calculations are as follows, where feed screw rotational speed is taken as 15 rev/min, and nozzle temperature is taken as 250 ^oC:

$$N_f = 15\ rev/min$$

$$T_c = 250\ ^oC$$

$$t = 100\ sec$$

M_{ec} = 1.2900 *gm* = mass of empty weigh cup

M_{fc} = 1.4569 *gm* = mass of aluminum cup with extruded ABS

$$M_{ABS-E} = M_{ec} - M_{fc} \tag{4.3.3}$$

$$M_{ABS-E} = 1.4569 - 1.2900 = 0.1669\ gm$$

Given the mass of extruded ABS together with its density, the volume of extruded material (V_{ABS-E})can be readily computed.

D_{ABS} = 1.04 gm/cm^3 = density of ABS plastic

$$V_{ABS-E} = \frac{M_{ABS}}{D_{ABS}} \tag{4.3.4}$$

$$V_{ABS-E} = {}^{0.1669}/_{1.04} = 0.16048\ cm^3$$

From these calculations, the actual volume of extruded ABS ($V_{ABS\text{-}E}$) produced at a given feed screw rotational speed during a 100 second interval was known. Similar calculations were conducted to determine the volume of ABS plastic being fed into the nozzle ($V_{ABS\text{-}In}$) for each filament feed rate (f_f).

It is straightforward to mathematically predict the volumetric flow rate of filament entering the extruder by multiplying the cross sectional area of filament (mm^2) by the linear feed rate (mm/sec). For a filament feed rate of f_f = 15 mm per minute and a filament radius of $r_{ABS\text{-}In}$ = 1.5 mm, the volumetric flow rate of material going into the extruder (Q_f) is:

$$Q_f = \pi \times (r_{ABS-In})^2 \times f_f \tag{4.3.5}$$

$$Q_f = \pi \times 1.5^2 \times 15 = 106.03 \; {}^{mm^3}/_{min} = 0.1060 \; {}^{cm^3}/_{min}$$

For a time span of t = 100 seconds, the volume of material fed into the heated extruder would be estimated as:

$$V_{ABS-In} = Q_f \times t$$

$$V_{ABS-In} = 0.1060 \; {}^{cm^3}/_{min} \times \frac{1 \; min}{60 \; sec} \times 100 \; sec = 0.1767 \; cm^3$$

Finally, the actual measured volume of extruded ABS exiting the nozzle can be compare with the predicted volume of ABS plastic fed into the nozzle at each given feed screw rotational speed. The percentage difference between these two numbers (Δ_V%) gives an indication of whether or not any losses in the extrusion mechanism exist. These losses mainly occur due to slippage between the feed screw and the filament. At high screw feeds, it is intuitively obvious that the plastic will not have sufficient time in the heated barrel to soften before it reaches the constriction point of the 0.5 mm diameter extrusion nozzle. These experiments are therefore useful at determining the upper limits of screw feed rates that are practical to use.

$$\Delta_V(\%) = \frac{V_{ABS-In} - V_{ABS-E}}{V_{ABS-In}} \times 100\% \tag{4.3.6}$$

$$\Delta_V \; (\%) = \frac{0.1767 - 0.1605}{0.1767} \times 100\% = 9.17 \; \%$$

Similar calculations were performed to find Δ_V for each feed screw feed and temperature combination. Results are reported in Table 5. In all cases, the predicted extrusion flow rate is higher than the actual extrusion flow rate. This is expected, because the mathematical predictions assume a 100% efficient feed mechanism with no losses due to slippage or backpressure. Although Table 5 shows some fluctuations in volumetric flow losses as a function of temperature, it is clear that the feed screw rotational speed has a pronounced effect. From 15 rev/min up to 100 rev/min feed screw speeds, the feed losses are relatively level. There are very pronounced jumps in feed losses going from 100 rev/min to 150 rev/min and from 150 rev/min up to 200 rev/min.

Table 5: Volumetric losses as a function of feed screw speed and extrusion temperature

Feed screw rotational speed (rev/min)	**Δ_V (%) at 250°C**	**Δ_V (%) at 260°C**	**Δ_V (%) at 270°C**
15	9.20	8.33	4.41
30	8.14	9.66	5.85
60	7.96	8.37	6.00
100	9.15	10.65	8.81
150	13.20	14.36	11.65
200	28.22	23.59	14.97

Further, the actual volumetric flow rate (Q_{Ext}) through extruder tip during a time interval of t seconds can be calculated with the help of known mass of extruded ABS ($M_{ABS\text{-}E}$) and density of ABS (D_{ABS}).

$$Q_{Ext} = \frac{{}^{M_{ABS-E}}/_{t}}{D_{ABS}} \times 60\, {}^{sec}/_{min} \tag{4.3.7}$$

$$Q_{Ext} = \frac{{}^{0.1669\, g}/_{100\, sec}}{{}^{1.04\, g}/_{cm^3}} \times 1000\, {}^{mm^3}/_{cm^3} \times 60\, {}^{sec}/_{min} = 96.288\, {}^{mm^3}/_{min}$$

In an idealized lossless extruder system, the expected volumetric flow rate from the nozzle (Q_{Exp}) should be equal to the filament feed rate going into the nozzle. This can be calculated by

converting volume of fed-in filament ($V_{ABS\text{-}In}$) during a given time interval t (sec) into a per minute volumetric flow rate.

$$Q_{EXP} = \frac{V_{ABS-In}}{t} \times 60\, {}^{sec}/_{min}$$

$$Q_{EXP} = \frac{0.17673 cm^3}{100\, sec} \times 1000\, {}^{mm^3}/_{cm^3} \times 60\, {}^{sec}/_{min} = 106.0425\, {}^{mm^3}/_{min}$$

Similar calculations were performed for each combination to compare the actual volumetric flow rate with the expected ideal volumetric flow rate. Table 6 shows the actual volumetric flow rates at three different nozzle temperatures (250°C, 260°C, and 270°C) along with ideal volumetric flow rate at various feed screw rotational speeds.

Table 6: Comparison of volumetric flow rate at different feed screw rotational speeds

Feed screw rotational speed (rev/min)	Idealized volumetric flow rate (mm^3/min)	Actual volumetric flow rate at 250°C (mm^3/min)	Actual volumetric flow rate at 260°C (mm^3/min)	Actual volumetric flow rate at 270°C (mm^3/min)
15	106.0425	96.2885	97.2115	101.3653
30	212.0850	194.8269	191.5961	199.6730
60	424.1700	390.4038	388.6730	398.7115
100	706.9500	642.2885	631.6730	644.6538
150	1060.4250	920.4808	908.1346	936.9230
200	1413.9000	1014.9231	1080.3461	1202.2500

With these calculations at hand, a regression equation was generated with the help of a software tool developed at Cornell University named Eureqa. Eureqa software tool uses parametric curve fitting of the data (http://www.nutonian.com/products/eureqa/). For this study, a regression equation was generated to correlate the actual volumetric flow rate (w) as a function of feed screw rotational speed (x) and extrusion nozzle temperature (y).

$$w = f\,(x, y) = 7.51\, x + 0.000189\, x^2 y - 0.0587\, x^2 - 19 \qquad (4.3.8)$$

The generated regression equation has an R^2 value (coefficient of determination) of 0.99 indicating that the equation is a good fit to the input data. Further, a graph was plotted to

visualize the relationship between feed screw rotational speed and volumetric flow rate. From Figure 7, it is evident that for higher feed screw rotational speed, expected volumetric flow rate is much higher as compared to actual volumetric flow rate at all three temperatures. Hence it can be said that losses in the extrusion mechanism due to slippage and backpressure increase, as expected, with an increase in feed screw rotational speed. Also it can be observed that, when the nozzle temperature is at 270 ^{o}C, the volumetric flow rate is slightly higher than it is at 260 ^{o}C. The same observation applies comparing the 260 ^{o}C and 250 ^{o}C extrusion conditions. So it can be said that as the nozzle temperature increases, volumetric flow rate also increases. This is intuitively logical in the sense that the ABS plastic softens more at higher temperatures.

Additionally, it can be concluded that from feed screw rotational speeds from 15 rev/min to roughly 65 rev/min, there is an approximately linear relationship between feed screw rotational speed and volumetric flow rate. For feed screw rotational speeds of 15, 30 and 60 rev/min, the actual volumetric flow rates at 250 ^{o}C, 260 ^{o}C and 270 ^{o}C do not vary significantly. It is therefore concluded that nozzle head temperature has relatively little effect on actual volumetric flow rate in comparison with the effect of feed screw rotational speeds of 15 to 60 rev/min. In order to validate these assumptions, the flow rate (w) output data for feed screw rotational speeds (x) of 15, 30 and 60 rev/min and heating chamber temperatures (y) of 250, 260 and 270^{o}C were analyzed with the help of Eureqa.

$$w = f(x, y) = 6.52\,x - 0.519 \tag{4.3.9}$$

As expected, the generated equation is independent of heating chamber temperature (y). Also the R^2 value (coefficient of determination) of this temperature independent equation is 0.99. From equation 3.6.9, it is evident that for feed screw rotational speeds in the 15 to 60 rev/min range, the volumetric flow rate is independent of nozzle temperature. Hence, for establishing a relationship between screw feed rotational speed and nozzle head translation speed during printing, the nozzle head temperature can be kept constant for subsequent experimentation.

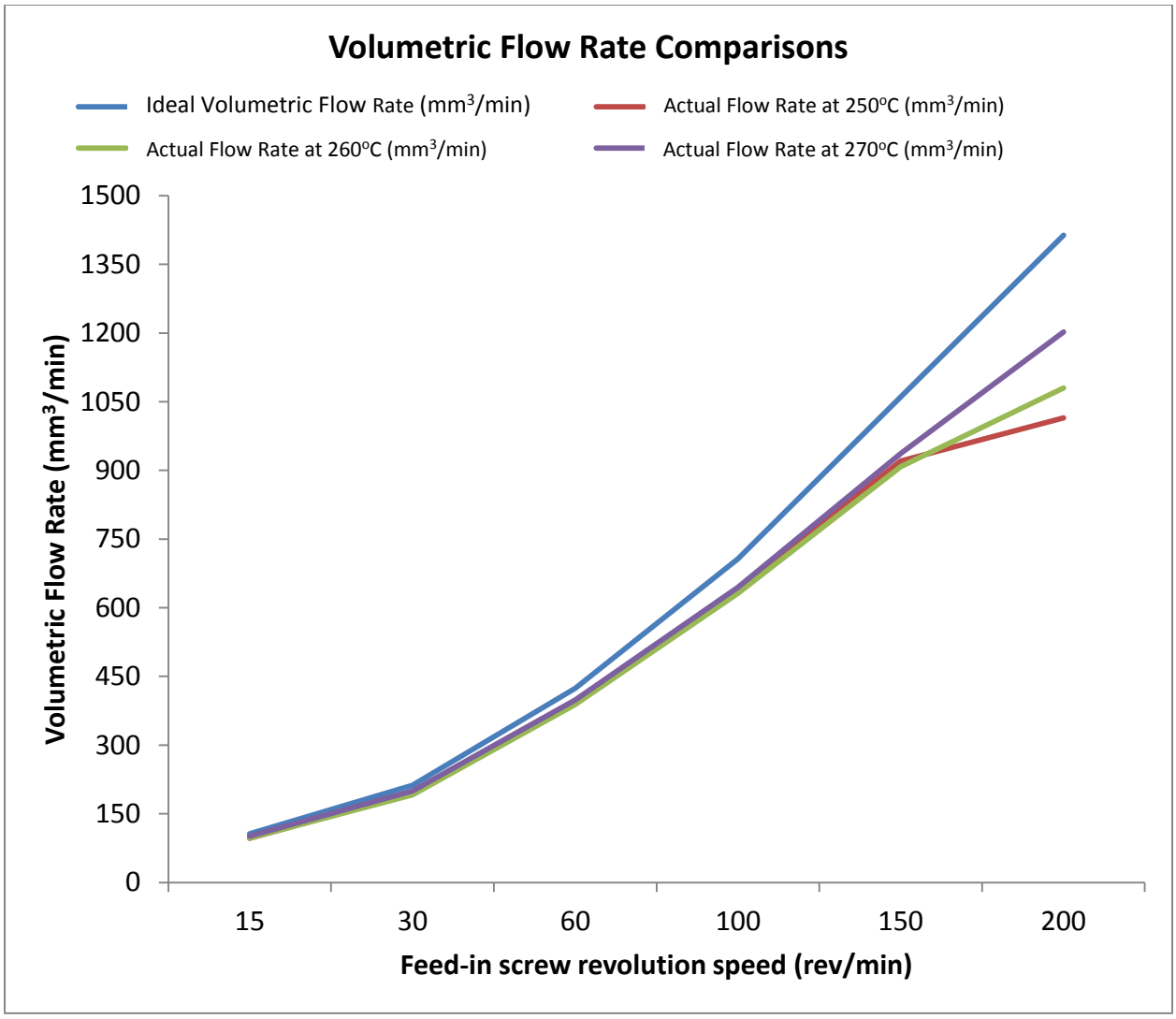

Figure 7: Volumetric flow rate versus feed screw speed and nozzle temperature

4.4 Relating feed screw rotational speed with nozzle head translation speed

One of the primary interests in high resolution 3D printing is to extrude lines that are as narrow as possible without breaking. At excessively slow nozzle translation speeds, material exits the nozzle faster than the nozzle is moving. Excess material accumulates beneath the nozzle and is therefore "smeared". At excessively high nozzle translation speeds, the extruded bead cannot keep up and is stretched to the breaking point. In order to find the right range of nozzle head translation speeds for each filament feed rate, straight lines were printed at various nozzle head translation speeds while keeping the feed rotational speed constant. Straight lines of 100

mm in length were printed for each sample. These straight lines were printed at three different feed screw rotational speeds (15, 30 and 60 rev/min). The temperature of the extrusion head was kept constant at 260 ^{o}C. The stand-off distance between the nozzle tip and substrate was kept at 0.500 mm based on observations during screening experiments in which smaller stand-off distances resulted in smearing of printed material and/or excessive back-pressure that clogged the nozzle.

Results from screen experiments were used to determine suitable ranges for nozzle head translation speeds. The nozzle head translation speed was kept approximately equal to the speed at which filament was expected to exit the nozzle based upon the feed screw rotational speed. By further looking at the quality of resulting printed lines, the nozzle head translation speeds were decreased and/or increased. For an extrusion head temperature of 260 ^{o}C and a feed screw rotational speed of 15 rev/min, a 100 mm/min nozzle head translation speed resulted in excessive material output relative to the translation speed of the nozzle (i.e. smearing). Hence for the 15 rev/min feed screw rotational speed, the nozzle head translation speed was increased in steps of 25 mm/min up to a speed of 300 mm/min. At a nozzle head translation speed of 300 mm/min, the printed line was very thin in width and barely stuck to the acrylic build platform. So for a 15 rev/min feed screw rotational speed, nozzle head translation speeds were varied between 100 mm/min and 300 mm/min in increments of 25 mm/min. A similar process was followed for 30 rev/min and 60 rev/min feed screw rotational speeds, and samples were printed. For the 30 rev/min feed screw rotational speed, nozzle head translation speeds were varied between 125 mm/min and 675 mm/min in increments of 50 mm/min. For the 60 rev/min feed screw rotational speed, nozzle head translation speeds were varied between 400 mm/min and 1300 mm/min in increments of 100 mm/min.

Printed lines were measured with the help of a Keyence IL-030 laser profilometer. Printed lines were located on the substrate, and the substrate was translated at a constant velocity of 0.5082 mm/sec. The spot size of the laser profilometer is given as 200 × 750 µm. The laser profilometer was mounted in such a way that the 0.2 mm beam spot dimension was scanned perpendicular to the printed line's axis to achieve the best possible resolution with this laser. The laser

profilometer was set capture a height reading every $1/10^{th}$ of a second and to record these values in an MS Excel spreadsheet. Each printed line was measured at three different locations to capture potential variability in line height or width. The measured height values for the three scans were averaged, and the standard deviation was calculated. Given a substrate velocity of 0.50882 mm/sec and a sampling frequency of $1/10^{th}$ of a second, the scan distance from one point to the next was 0.05082 mm. Also as we know the velocity of substrate (Laser scanning velocity – V_{Scan}) and the time required for scanning (t_{Scan}) the printed line, we can calculate the width of the printed line (W_{Line}). The following illustration shows how the width of printed line was computed.

$$W_{Line} = V_{Scan}\, X\, t_{Scan} \qquad (4.4.1)$$

$$V_{Scan} = 0.5082\ mm/sec$$

$$t_{Scan} = 1.3\ seconds$$

$$W_{Line} = 0.5082 \times 1.3 = 0.6607\ mm$$

Table 7 shows the average height readings for a feed screw rotational speed of 15 rev/min and a nozzle head translation speed of 300 mm/min.

A representative graph showing width (mm) vs. average height (mm) of a printed line is shown in Figure 8. The X and Y axes have the same scale to provide an accurate scale representation of height-to-width ratio. Similar graphs were plotted for every combination of feed screw rotational speed and nozzle head translation speed and can be found in Appendix B.

Table 7: Sample calculations for area under the curve for feed screw rotational speed of 15 rev/min and nozzle head translation speed of 300 mm/min

Time (sec)	Scan Location (mm)	Measured Height Location #1 (mm)	Measured Height Location #2 (mm)	Measured Height Location #3 (mm)	Average Height (mm)	Standard Deviation	Area under the curve (mm^2)
0.00	0.0000	0.000	0.000	0.000	0.000	0.000	0.00000
0.10	0.0508	0.144	0.096	0.120	0.120	0.020	0.00609
0.20	0.1016	0.195	0.156	0.175	0.175	0.016	0.00890
0.30	0.1525	0.247	0.207	0.226	0.226	0.016	0.01150
0.40	0.2033	0.290	0.243	0.254	0.262	0.020	0.01333
0.50	0.2541	0.296	0.239	0.263	0.266	0.023	0.01353
0.60	0.3049	0.269	0.231	0.266	0.256	0.017	0.01299
0.70	0.3557	0.266	0.221	0.256	0.248	0.019	0.01259
0.80	0.4066	0.266	0.224	0.258	0.249	0.018	0.01266
0.90	0.4574	0.241	0.206	0.238	0.228	0.016	0.01161
1.00	0.5082	0.213	0.181	0.202	0.199	0.013	0.01010
1.10	0.5590	0.254	0.208	0.220	0.227	0.020	0.01155
1.20	0.6098	0.332	0.272	0.285	0.296	0.026	0.01505
1.30	0.6607	0.000	0.000	0.000	0.000	0.000	0.00000
						Total Area under the curve	**0.13990**

The area under any given laser scan curve represents the cross sectional area of a printed line. In order to calculate this area, the laser step-over distance for each measurement was multiplied by the measured height at that step as illustrated in Figure 8. The total area under the curve was calculated as the summation of the individual areas. With a known area under the curve (A_C) and known nozzle head translation speed (V_S), the volumetric flow rate (Q_{EST}) was calculated by multiplying the two. The following calculations show the computation of volumetric flow rate for a feed screw rotational speed of 15 rev/min and a nozzle head translation speed of 300 mm/min.

$$Q_{EST} = A_C \times V_S \tag{4.4.2}$$

$$A_C = 0.1399\ mm^2$$

$$V_S = 300\ mm/min$$

$$Q_{EST} = 0.1399 \times 300 = 41.97\ mm^3/min$$

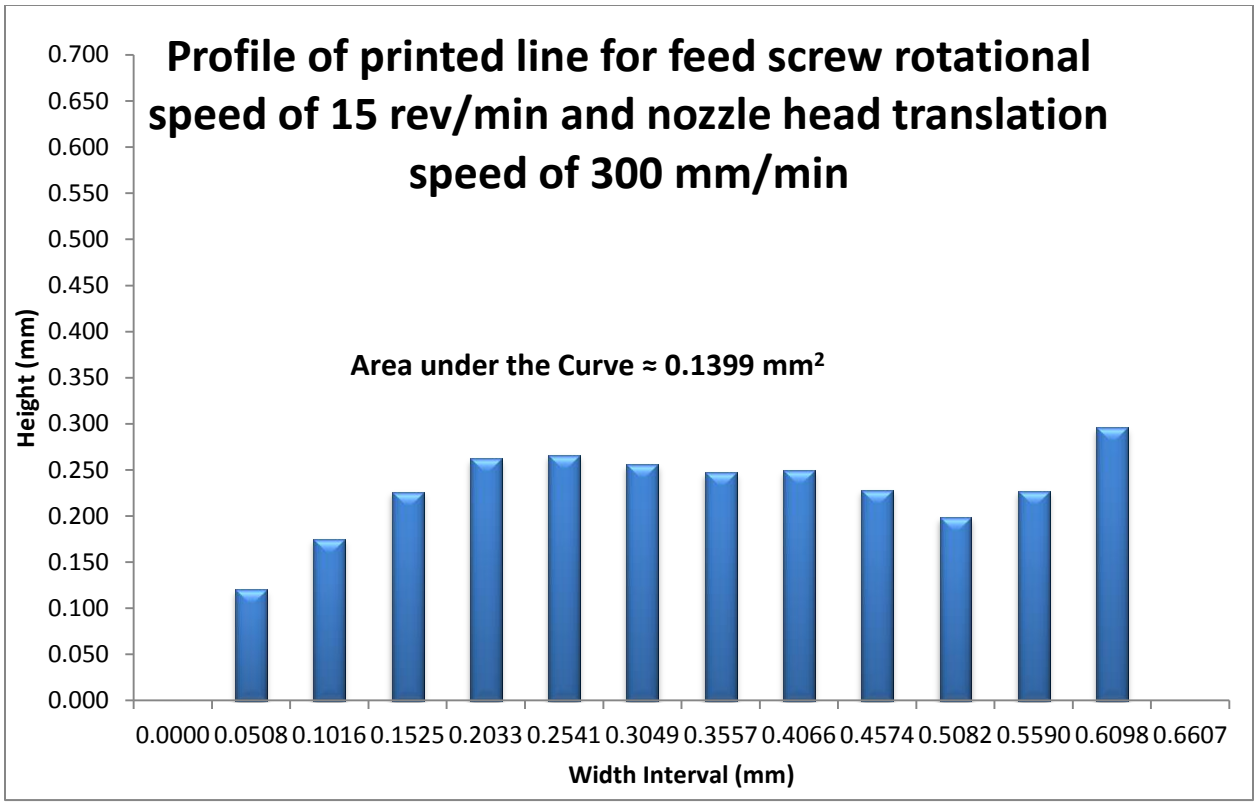

Figure 8: Cross-sectional profile of a printed line

Similar calculations were conducted for each nozzle head translation speed while keeping feed screw rotational speed constant. Table 8 shows the average height and width of printed lines at different head translation speeds with a feed screw rotational speed of 15 rev/min. Figure 9 graphically displays cross sectional area of printed lines as a function of nozzle head translation speed at a feed screw rotational speed of 15 rev/min.

Table 8: Nozzle head translation speed versus volumetric flow rate at 15 rev/min feed screw speed

Nozzle head Translation Speed (mm/min)	Average Measured Height (mm)	Average Measured Width (mm)	Cross Sectional Area (mm^2)	Calculated Volumetric Flow Rate (mm^3/min)
100	0.5104	2.5918	1.2970	129.6955
125	0.4496	1.7279	0.7540	94.2517
150	0.2959	1.8295	0.5264	78.9573
175	0.3111	1.7787	0.5375	94.0687
200	0.2888	1.4738	0.5016	100.3220
225	0.2871	0.5590	0.1459	32.8275
250	0.2658	0.6098	0.1486	37.1474
275	0.2856	0.5082	0.1306	35.9263
300	0.2294	0.6607	0.1399	41.9690

While printing, it was observed that for relatively low nozzle head translation speeds of 100 and 125 mm/min, the nozzle smeared the printed material. This suggests that the head translation speed was too slow in relation to the velocity at which material was exiting the nozzle. As shown in the printed line photographs in Figure 9, this significantly increases the width of the printed lines. This can also lead to trapped air in the printed samples or excessive back pressure that inhibits flow of material from the nozzle. In order to avoid this condition, a nozzle head translation speed of at least 150 mm/min is recommended for the 15 rev/min feed screw rotational speed. Figure 9 also shows that at higher nozzle head translation speeds, the line width becomes thinner and thinner.

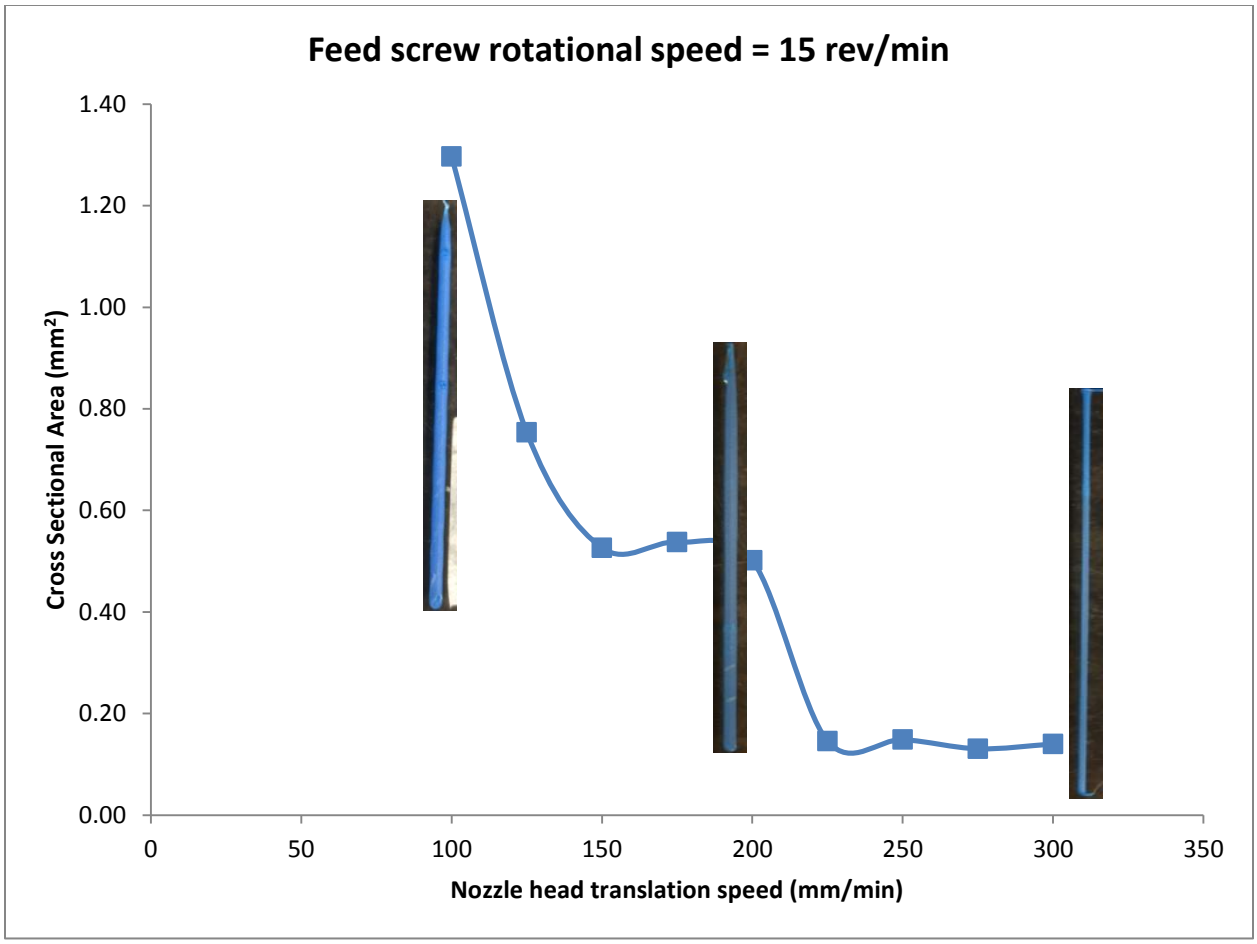

Figure 9: Cross-sectional area vs. nozzle head translation speed at 15 rev/min feed screw speed

A similar analysis was conducted for a feed screw rotational speed of 30 rev/min. Table 9 shows the average height and width of printed lines and calculates the volumetric flow rate at each nozzle translation speed.

Table 9: Nozzle head translation speed versus volumetric flow rate at 30 rev/min feed screw speed

Nozzle head Translation Speed (mm/min)	Average Measured Height (mm)	Average Measured Width (mm)	Cross Sectional Area (mm^2)	Calculated Volumetric Flow Rate (mm^3/min)
175	0.3124	1.2197	0.3651	63.8970
225	0.2947	1.3721	0.3894	87.6165
275	0.2758	1.3721	0.3644	100.1998
325	0.3154	1.3213	0.4007	130.2429
375	0.2641	1.4738	0.3758	140.9302
425	0.2860	1.2197	0.3343	142.0896
475	0.2843	1.2705	0.3467	164.7005
525	0.2762	1.1180	0.2947	154.7272
575	0.3194	0.9148	0.2714	156.0615
625	0.4070	0.6098	0.2275	142.1991
675	0.2500	0.9148	0.2124	143.3683

Figure 10 displays cross-sectional area versus nozzle head translation speed for a feed screw rotational speed of 30 rev/min. A similar effect of reduction in line width was observed when nozzle head translation speed was increased.

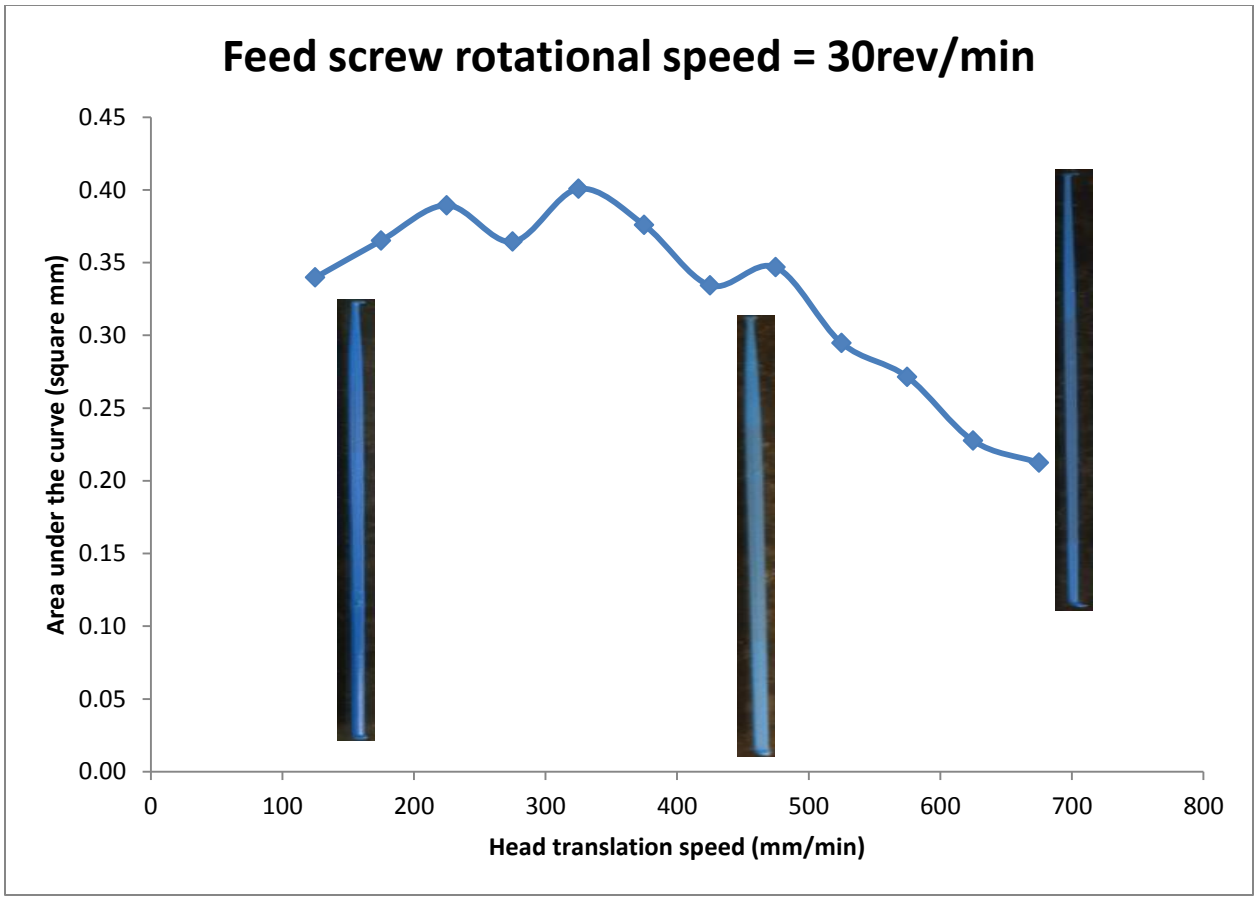

Figure 10: Cross-sectional area vs. nozzle head translation speed at 30 rev/min feed screw speed

Table 10 shows the average height and width of the printed line at 60 rev/min feed screw rotational speed and calculates the volumetric flow rate with the help of area under the curve.

Table 10: Nozzle head translation speed versus volumetric flow rate at 60 rev/min feed screw speed

Nozzle head Translation Speed (mm/min)	Average Measured Height (mm)	Average Measured Width (mm)	Cross Sectional Area (mm^2)	Calculated Volumetric Flow Rate (mm^3/min)
400	0.3858	2.2361	0.8430	337.2092
500	0.3234	2.0328	0.6409	320.4376
600	0.3164	1.7279	0.5307	318.4202
700	0.2958	1.8295	0.5262	368.3461
800	0.2950	1.5246	0.4348	347.8542
900	0.2261	1.5246	0.3332	299.9075
1000	0.2031	1.5754	0.3063	306.3133
1100	0.1664	1.4230	0.2283	251.1592
1200	0.1203	1.4738	0.1712	205.4175
1300	0.0923	1.4230	0.1267	164.6731

Figure 11 displays cross-sectional area versus nozzle head translation speed at a feed screw rotational speed of 60 rev/min. At a translation speed of 400 mm/min, excessive material flow in relation to translation speed is evident from the photographs. As a result, the printed line was disrupted leading to wider width. As the nozzle head translation speed increases, the line width reduces which can also be noticed in the width of the printed lines. At 60 rev/min feed screw rotational speed, the measured volumetric flow rate was 388.573 mm^3/min.

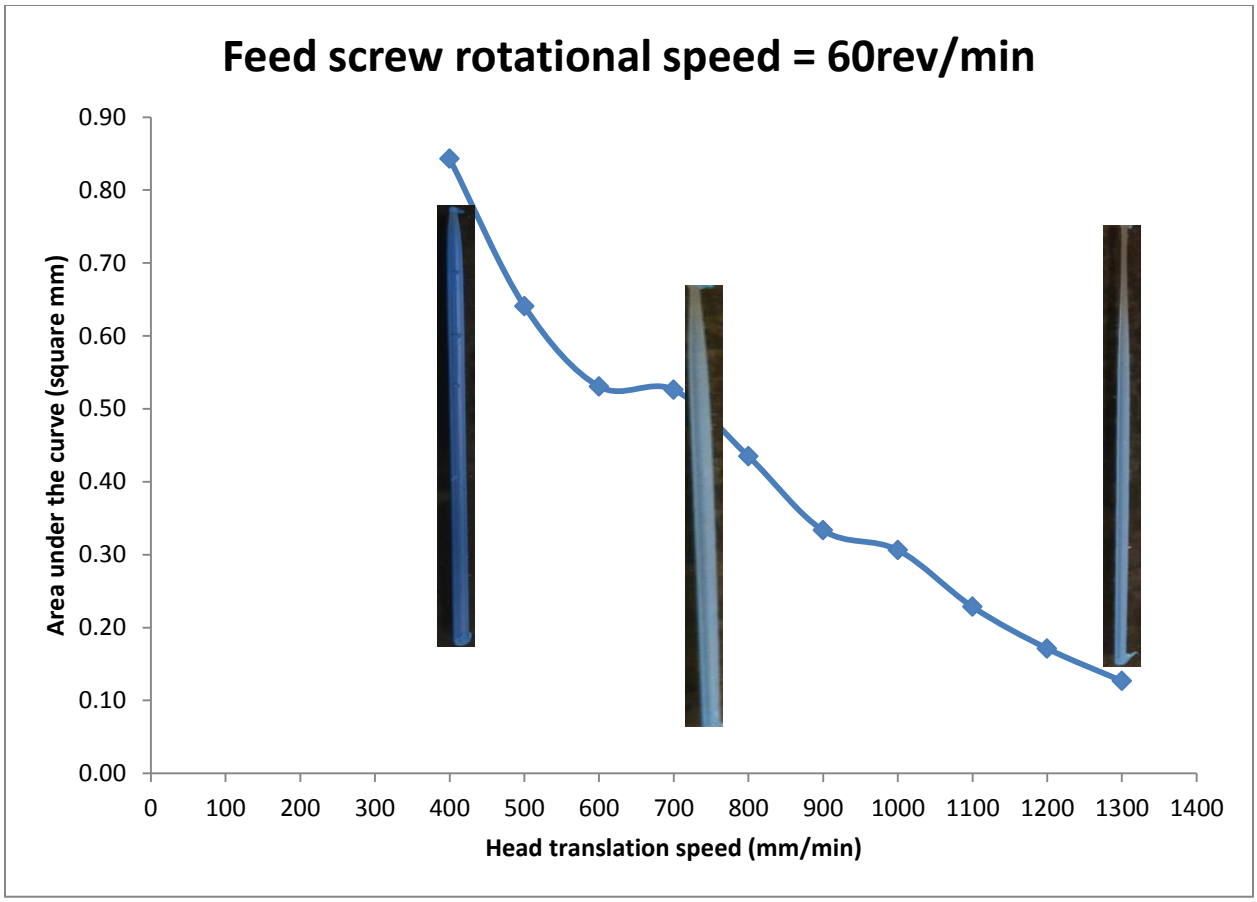

Figure 11: Cross-sectional area vs. nozzle head translation speed at 60 rev/min feed screw speed

From these experiments, the conditions under which excessive extruded in relation to translation speed was observed. However, there were conditions under which smearing of the printed line by the nozzle was observed even when the translation speed theoretically matched the velocity of material exiting the nozzle. It was hypothesized that this was due to the die swell phenomenon in which extruded material swells to a certain degree upon exiting the nozzle due to recoverable strain. If the diameter of the printed bead increases, then that suggests that it would be necessary to increase the stand-off distance between build platform and nozzle tip in order to avoid smearing the larger diameter bead of plastic. In order to find the optimal stand-off distance, it was necessary to find the diameter of extruded filament. The diameter of nozzle tip used in these trials was 0.5 mm. A series of experiments were therefore conducted to assess the degree of die swell relative to the 0.5 mm nozzle diameter.

4.5 Die swell phenomenon in FFE

Die swell is a common phenomenon in an extrusion process. When the viscous fluid flows through the small orifice, the extruded diameter is usually greater than the diameter of the orifice. This phenomenon is referred to as the die swell effect. In the heated nozzle of an FFE machine, the softened 3 mm diameter filament is forced through a 0.5 mm diameter nozzle opening. This imparts high shear strain upon the polymer. The viscoelastic polymer will have a certain amount of recoverable strain upon exiting the nozzle, resulting in expansion of the bead of plastic. The amount of recoverable strain is generally influenced by the amount of time the polymer resides in the heated nozzle. The longer the material is in the nozzle, the more it "relaxes" and loses its recoverable strain. Intuitively, one would therefore expect to see more die swell in the FFE process as the feed screw speeds increase. Put another way, the diameter of the extruded bead would be expected to increase at higher feed rates because the polymer spends less time in the extruder.

In order to study this phenomenon, the extruded samples reported in Section 4.3 were used. These samples were extruded at three different extrusion head temperatures of 250^{o}C, 260^{o}C and 270^{o}C; and at feed screw rotational speeds of 15, 30, 60, 100, 150 and 200 rev/min. The diameter of each extruded sample was measured at eight different locations using digital vernier calipers, and the average diameter of the extruded filament was used as the response value. Table 11 shows the average measured diameter for the combination of each feed screw rotational speed and nozzle temperature. In order to visualize the effect of nozzle temperature and feed screw rotational speed on the diameter of extruded filament, the 3D graph shown in Figure 12 was prepared.

Table 11: Measured diameter of extruded ABS versus feed screw speed and nozzle temperature

Diameter of extruded ABS (mm)		Nozzle temperature (°C)		
		250°C	260°C	270°C
Feed screw rotational speed (rev/min)	15	0.586	0.558	0.549
	30	0.610	0.615	0.628
	60	0.676	0.671	0.685
	100	0.816	0.785	0.754
	150	0.999	0.929	0.929
	200	1.036	0.975	0.976

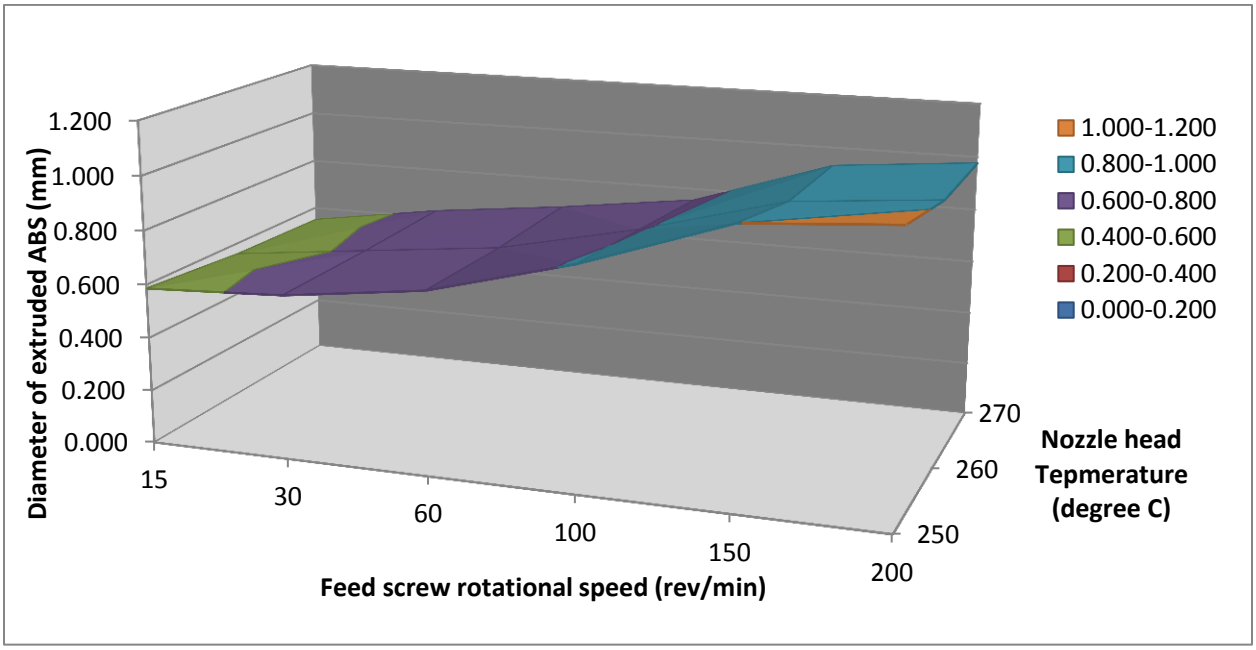

Figure 12: Diameter of extruded ABS vs. feed screw rotational speed and nozzle temperature

It is clear from the graph that for a given nozzle temperature, the diameter of extruded filament increases substantially as the feed screw rotational speed increases. This experimental observation agrees with expectations, since at higher feed rates, then melt spends less time in the heated nozzle and will therefore have higher recoverable strain. The magnitude of die swell is quite remarkable though. As feed screw speed increases from 15 rev/min to 150 rev/min, the filament diameter jumps from 0.586 mm up to 0.999 mm. This almost doubling of filament

diameter has significant ramifications for the recommended gap size between the nozzle and substrate.

Now if one considers a constant feed screw rotational speed, there is a minor reduction in extruded filament diameter as the nozzle temperature increases. This also makes intuitive sense, as the polymer becomes softer at higher temperatures and will lose recoverable strain. Compared with the effect of filament feed rate, however, the effect of temperature on the die swell effect is negligible.

These experiments suggest that the nozzle gap distance must be increased or decreased as the filament feed rate changes in order to account for changes in the diameter of the extruded material. Failure to do so can result in smearing of the printed material if the gap distance is smaller than the extruded bead diameter. If the gap distance is larger than the bead diameter, than the extruded bead may fail to attach to the substrate.

4.6 Validation

A validation experiment was conducted to verify and correlate the die swell effect on the FFE process. In order to conduct the validation experiment for each feed screw rotational speed, the stand-off distance and nozzle head translation speed were varied while keeping the nozzle temperature constant at 260^{o}C. The stand-off distance was set equal to the extruded bead diameter experimentally determined and reported in Table 11. Table 12 shows the process parameters for the validation experiment.

Table 12: Process parameters for validation experiment

Feed screw rotational speed (rev/min)	Stand-off distance (mm)	Nozzle head translation speed (mm/min)
15	0.56	200
30	0.62	475
60	0.67	700

Using the process parameters settings as shown in Table 12, 100 mm long straight lines were printed. The laser profilometer measurement procedure described in Section 4.4 was used to measure width and height of the printed lines as well as the cross sectional profile. Table 13

shows the predicted and calculated cross sectional areas for each sample. The validation results show very good agreement between the expected and actual measured cross sectional areas. This indicates that the modified stand-off distances successfully accounted for the die-swell effects as the filament feed rate increases.

Table 13: Results of the validation experiment

Feed screw rotational speed (rev/min)	Nozzle translation speed (mm/min)	Stand-off distance (mm)	Expected cross sectional area (mm^2) = πr^2	Calculated cross sectional area (mm^2)
15	200	0.56	0.2463	0.2520
30	475	0.62	0.3019	0.2961
60	700	0.67	0.3526	0.3500

5 Conclusions and Recommendations

5.1 Conclusions

One of the stated research objectives for this work was to establish a process to find suitable nozzle head translation speeds for a given feed screw rotational speed. The aim is to avoid excessive of insufficient extruded filament volume in relation to the nozzle translation speed. Through screening experiments conducted on an open-source BFB-3000 FFE machine, examples of excessive and insufficient filament material flow were observed. It was concluded that for feed screw rotational speeds ranging from 15 rev/min to 60 rev/min, the volumetric flow rate is essentially independent of extrusion nozzle temperature for ABS plastic. Furthermore, an essentially linear relationship between feed screw rotational speed and volumetric flow rate was observed for this feed screw rotational speed range. This indicated that minimal slippage between the feed screw and filament existed within this range.

A second accomplishment was that filament extrusion velocities were correlated with feed screw rotational speeds in order to determine suitable nozzle head translation speeds for the BfB-3000 FFE machine. By correlating filament feed rate with the velocity that filament exits the nozzle, it is possible to either:

a) Determine the nozzle translation speed during printing that should be used for a given filament feed rate; or
b) Determine the filament feed screw speed that should be used for a desired nozzle translation speed.

A significant die swell effect was observed in the FFE process. As the feed screw rotational speed was increased, the diameter of the extruded filament also increased. At high screw feeds, the diameter nearly doubled, hence this is not a minor process variation that can be ignored. It was further observed that the effect of nozzle temperature on the magnitude of die swell was negligible. The die swell effect must be understood and accounted for in with respect to the layer thickness. If the diameter of the filament exiting the nozzle exceeds the gap

between the nozzle and substrate (which equals layer thickness), then the nozzle smears the printed bead of material. In order to avoid this, one must either:

a) Increase or decrease the stand-off distance (i.e. layer thickness) as the filament feed rate is increased or decreased to compensate for the changing extrusion bead diameter; or
b) Set the filament feed rate at a value that produces a bead diameter compatible with the desired layer thickness.

Last column in the table 15 indicates the suggested stand-off distance in order to avoid piling up of an extruded filament. The stand-off distance values are nothing but the measured diameter values of an extruded ABS filament from 0.5 mm nozzle diameter when heating chamber temperature is 260^{o}C.

Taking everything that has been learned, and summarizing it in a single table (Table 15), we can determine the minimum and maximum recommended values for nozzle head translation speeds for a given feed screw rotational speed.

Feed in rate (rev/min)	Minimum nozzle head translation speed (mm/min)	Maximum nozzle head translation speed (mm/min)	Suggested stand-off distance (mm)
15	150	250	0.56
30	375	575	0.62
60	600	800	0.67

Table 14: Suggested nozzle head translation speed range and stand-off distance for each feed screw rotational speed

5.2 Future Work

The entire work in this thesis was focused on an open-source BFB-3000 system that has been built primarily for the hobby and educational markets. The process described can be replicated

to determine extruded filament diameters, filament feed rates, and recommended nozzle translation speeds for other thermoplastics of interest such as PLA, polycarbonate, nylon, etc.

As it is known that different filament feed rates produce dramatically different extruded bead diameters, this fact can potentially be used to improve part quality and/or build speeds. For example, adaptive slicing techniques can be used in which very thin contours are printed to produce fine surface finish, while thick infill layers are printed to more rapidly produce the part (i.e. thicker layers means fewer layers to print and therefore less build time). If the layer thickness is intentionally set less than the bead diameter, then a small amount of smearing of the bead can be desirable in terms of producing higher density parts with fewer gaps between adjacent printed traces.

6 References

Ahn, D., Kweon, J. H., Kwon, S., Song, J., & Lee, S. (2009). Representation of surface roughness in fused deposition modeling. *Journal of Materials Processing Technology, 209*(15), 5593-5600.

Ahn, S. H., Montero, M., Odell, D., Roundy, S., & Wright, P. K. (2002). Anisotropic material properties of fused deposition modeling ABS. *Rapid Prototyping Journal, 8*(4), 248-257.

Bellini, A., & Güçeri, S. (2003). Mechanical characterization of parts fabricated using fused deposition modeling. *Rapid Prototyping Journal, 9*(4), 252-264.

Chua, C. K., Leong, K. F., & Lim, C. S. (2010). *Rapid prototyping: principles and applications*: World Scientific Pub Co Inc.

Galantucci, L., Lavecchia, F., & Percoco, G. (2009). Experimental study aiming to enhance the surface finish of fused deposition modeled parts. *CIRP Annals-Manufacturing Technology, 58*(1), 189-192.

Han, W., Jafari, M. A., & Seyed, K. (2003). Process speeding up via deposition planning in fused deposition-based layered manufacturing processes. *Rapid Prototyping Journal, 9*(4), 212-218.

Helmer, W., & Mobbs, D. (2011). *An Evaluation of Some Low-cost Rapid Prototyping Systems for Educational Use*.

Hoekstra, N. L., Pennington, R. C., & Newcomer, J. L. (2005). Significant factors in the Dimensional Accuracy of Fused Deposition Modeling. *Proceedings of the Institution of Mechanical Engineers. Part E, Journal of Process Mechanical Engineering, 219*(1), 89-92.

Lee, C., Kim, S., Kim, H., & Ahn, S. (2007). Measurement of anisotropic compressive strength of rapid prototyping parts. *Journal of materials processing technology, 187*, 627-630.

Masood, S. H. (1996). Intelligent rapid prototyping with fused deposition modelling. *Rapid Prototyping Journal, 2*(1), 24-33.

Pandey, P. M., Venkata Reddy, N., & Dhande, S. G. (2003). Improvement of surface finish by staircase machining in fused deposition modeling. *Journal of materials processing technology, 132*(1), 323-331.

Pham, D., & Gault, R. (1998). A comparison of rapid prototyping technologies. *International Journal of Machine Tools and Manufacture, 38*(10-11), 1257-1287.

Saqib, S., & Urbanic, J. (2012). An Experimental Study to Determine Geometric and Dimensional Accuracy Impact Factors for Fused Deposition Modelled Parts. *Enabling Manufacturing Competitiveness and Economic Sustainability*, 293-298.

Sood, A. K., Ohdar, R., & Mahapatra, S. (2009). Improving dimensional accuracy of Fused Deposition Modelling processed part using grey Taguchi method. *Materials & Design, 30*(10), 4243-4252.

Sood, A. K., Ohdar, R. K., & Mahapatra, S. S. (2012). Experimental investigation and empirical modelling of FFE process for compressive strength improvement. *Journal of Advanced Research, 3*(1), 81-90.

Vasudevarao, B., Natarajan, D. P., Henderson, M., & Razdan, A. (2000). *Sensitivity of RP surface finish to process parameter variation*.

Yan, X., & Gu, P. (1996). A review of rapid prototyping technologies and systems. *Computer-Aided Design, 28*(4), 307-318.

Yang, Y., Fuh, J. Y. H., Loh, H. T., & Wong, Y. S. (2003). Multi-orientational deposition to minimize support in the layered manufacturing process. *Journal of manufacturing systems, 22*(2), 116-129.

Appendix A: BFB Machine Codes

M101 // Turn on extruder 1 (Feed screw rotational speed equal to previous M108 command)

M201 // Turn on extruder 2 (Feed screw rotational speed equal to previous M108 command)

M103 // Turn off all extruders

M104 S260 // Set Extruder 1 temperature to 260^{o}C

M108 S600 //Set Extruder 1 feed-in rev/min to (S value/10) = 60 rev/min

G1 X40 Y10 Z5 F480 // Move nozzle head to coordinates X = 40 mm, Y = 10 mm and Z = 5 mm with the translation speed of 480 mm/min (F value)

Appendix B: Profile of printed lines

B1: Profile of printed lines for feed screw rotational speed of 15 rev/min and variable nozzle head translation speed

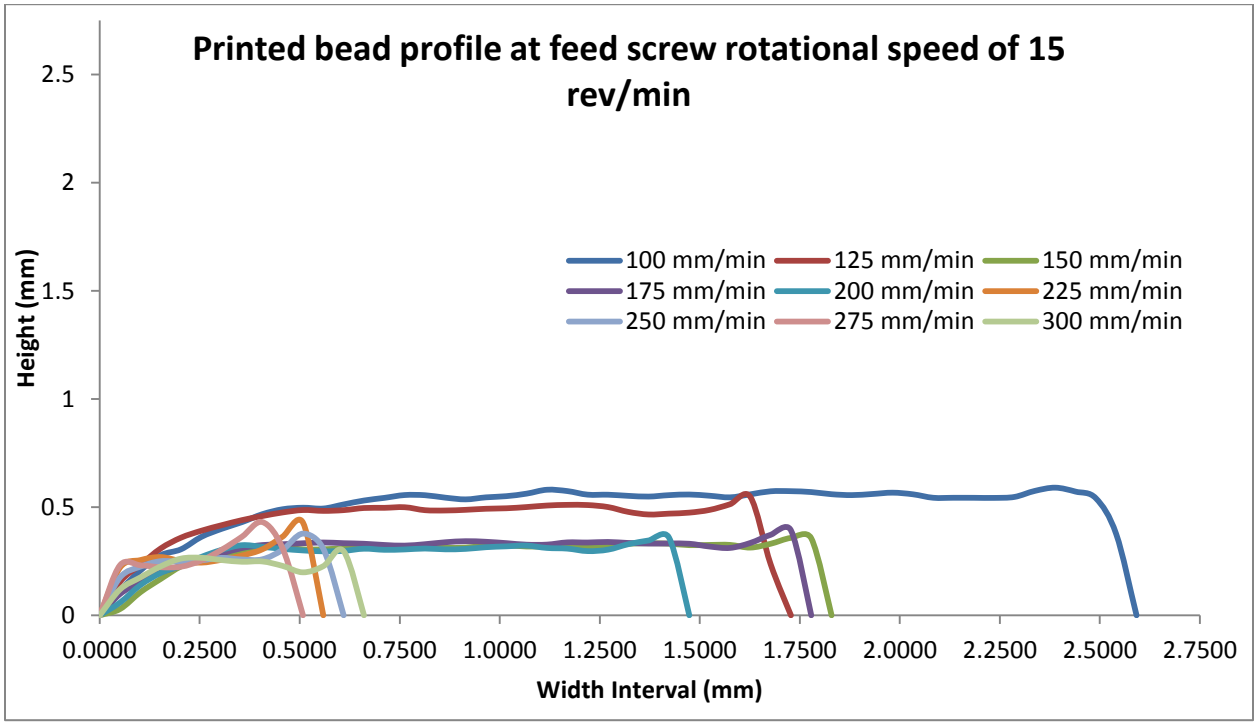

B2: Profile of printed lines for feed screw rotational speed of 30 rev/min and variable nozzle head translation speed

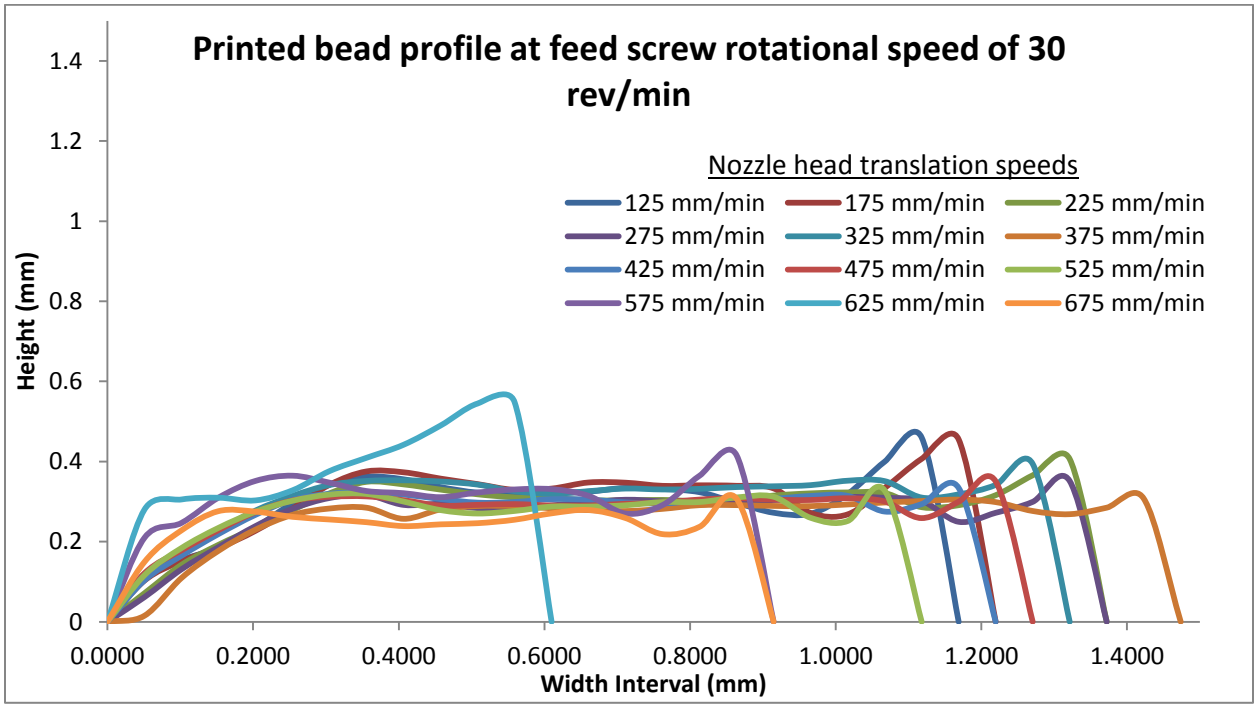

B3: Profile of printed lines for feed screw rotational speed of 60 rev/min and variable nozzle head translation speed